



ARTICLE

# A Generative Model-Based Network Framework for Ecological Data Reconstruction

Shuqiao Liu<sup>1</sup>, Zhao Zhang<sup>2,\*</sup>, Hongyan Zhou<sup>1</sup> and Xuebo Chen<sup>1</sup>

<sup>1</sup>School of Electronic and Information Engineering, University of Science and Technology Liaoning, Anshan, 114051, China

<sup>2</sup>School of Computer Science and Software Engineering, University of Science and Technology Liaoning, Anshan, 114051, China

\*Corresponding Author: Zhao Zhang. Email: zhangzhao@ustl.edu.cn

Received: 14 August 2024 Accepted: 24 October 2024 Published: 03 January 2025

## ABSTRACT

This study examines the effectiveness of artificial intelligence techniques in generating high-quality environmental data for species introductory site selection systems. Combining Strengths, Weaknesses, Opportunities, Threats (SWOT) analysis data with Variation Autoencoder (VAE) and Generative Adversarial Network (GAN) the network framework model (SAE-GAN), is proposed for environmental data reconstruction. The model combines two popular generative models, GAN and VAE, to generate features conditional on categorical data embedding after SWOT Analysis. The model is capable of generating features that resemble real feature distributions and adding sample factors to more accurately track individual sample data. Reconstructed data is used to retain more semantic information to generate features. The model was applied to species in Southern California, USA, citing SWOT analysis data to train the model. Experiments show that the model is capable of integrating data from more comprehensive analyses than traditional methods and generating high-quality reconstructed data from them, effectively solving the problem of insufficient data collection in development environments. The model is further validated by the Technique for Order Preference by Similarity to an Ideal Solution (TOPSIS) classification assessment commonly used in the environmental data domain. This study provides a reliable and rich source of training data for species introduction site selection systems and makes a significant contribution to ecological and sustainable development.

## KEYWORDS

Convolutional Neural Network (CNN); VAE; GAN; TOPSIS; data reconstruction

## 1 Introduction

Currently, with the rapid development of deep learning data processing technology, its powerful data representation ability is also widely welcomed in the field of sustainable development and environmental development [1]. However, training deep neural networks requires a large amount of annotated data, but many of the current ecosystem development data suffer from thin data volumes and difficulties in data access. In addition, ecological data have large differences in positive and negative categories, making it difficult to annotate and uniformly train them. In order to address the above issues, a network framework that combines Strengths, Weaknesses, Opportunities, and Threats



(SWOT) analysis data with Variation Autoencoder (VAE) and Generative Adversarial Network (GAN) networks (SAE-GAN). The framework also references the Technique of Similarity Ordering Preferences for Ideal Solutions (TOPSIS) detection, which synthesizes to provide a practical solution.

Many well-established models and frameworks exist that can provide references to ambient modal to textual data [2], as well as read parameters and transfer information efficiently and accurately [3]. Among them, data generation models, such as GAN and VAE, have been proposed for various tasks (For example, the process of image ecological change [4], Information extraction and species prediction [5–7], Species and Scene Detection [8,9]). Recently, some studies [10] have also used generative modeling [11] to deal with the problem of environmental sequence data generation. To fully utilize their potential, our generative model SAE-GAN takes advantage of GAN and VAE to generate features that expand the analyzed data with the help of integrating the analyzed data as conditional information. It should be noted that existing studies [12,13] have demonstrated the effectiveness of generative models to simulate input data. In order to address the problem of large differences between positive and negative categories in ecological data, we creatively use SWOT analysis data to replace the original collection data, and the framework integration of SWOT analysis is more conducive to the comprehensive assessment of the data.

Our aim is to expand the dataset in order to fully utilize the existing data for analytical prediction, where Autoencoder (AE) as well as the extended VAE model have been fully validated for their accuracy in generating new samples for the data [13]. And among them, VAE has even better data extraction ability due to the known nature of its potential space. Meanwhile, although GAN is a powerful generative model and is often used to generate new similar data [14], it suffers from the problems of unstable training and low quality of generated samples. Different methods have been proposed to improve GAN, such as Wasserstein GAN (WGAN) [15] and Deep Convolutional (DCGAN) [16], which have achieved certain superior results. In this paper, after comprehensive comparison experiments, it is verified that VAE add GAN together have better results in the field of data generation, and VAE can better accomplish sample generation and adjustment through its potential space for differencing and control. When combined with GAN, an adversarial training mechanism can be introduced into the latent space to further optimize sample generation. The reparameterization technique of VAE makes the training process more efficient, while GAN improves the generative ability through the adversarial mechanism. The combination of the two can complement each other's deficiencies and improve the overall training efficiency. This study will provide a comprehensive overview of the architecture and training procedures of the SAE-GAN model, as well as an assessment of the accuracy and value of the generated synthetic data. The results of this study can provide a reliable and rich source of training data for species introduction site selection systems, thus making a significant contribution to ecological and even sustainable development.

By creating high-quality, contextually accurate synthetic data, we can overcome the limitations of existing datasets while improving the accuracy of species siting models. This study will provide an in-depth analysis of the design, training procedures, and general efficacy of VAEs and GANs to generate synthetic data. We will also conduct a comprehensive evaluation of the generated synthetic data, using a variety of metrics and experiments to assess its quality and usefulness. The potential impact of this study is enormous, offering a promising solution to the data shortage.

Fig. 1 illustrates the general framework of our conditional generation model, which is an intuitive combination of Missing importance weighted autoencoder (MIWAE) and GAN. In addition to the regular encoder (E), the generator (G), and the discriminator (D), we use the SWOT analysis data as inputs to incorporate sample factor classification sampling merged into our model to ensure that

the generated features are discriminable at the category level. Specifically, our model consists of four components, namely, Encoder E, Generator G, Discriminator D, and Categorizer C. Our model is trained based on the seen class features and their corresponding class-level semantic embeddings. After 3 training sessions, our model can generate high-quality features for unseen classes and give the corresponding semantic embedding.

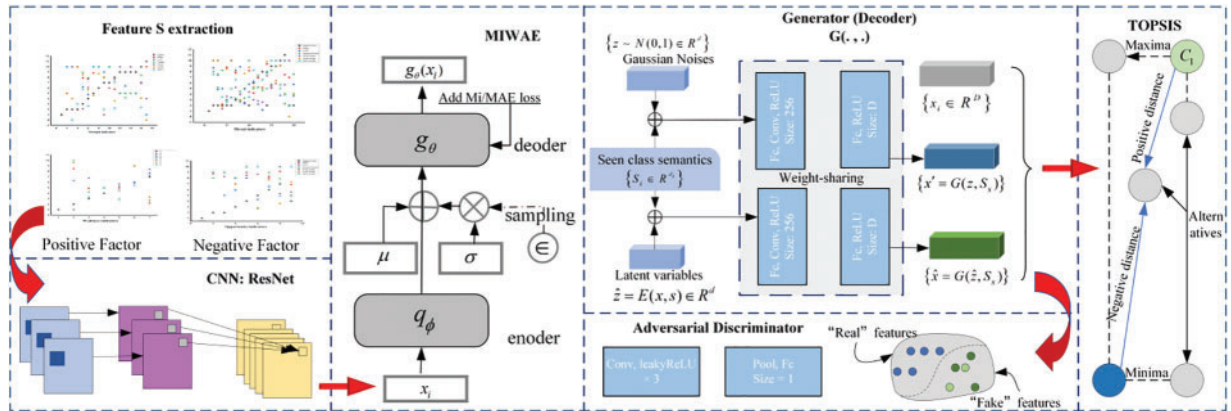


**Figure 1:** Illustration of our joint generative model (SWOT-MIWAE-GAN)

Meanwhile, we employ perceptual reconstruction to retain more semantic information for feature generation. The proposed joint generation model can mitigate the domain drift problem by generating features similar to the actual distribution, which is robust and generalizable to the data reconstruction task. The specific structure is shown in Fig. 2.

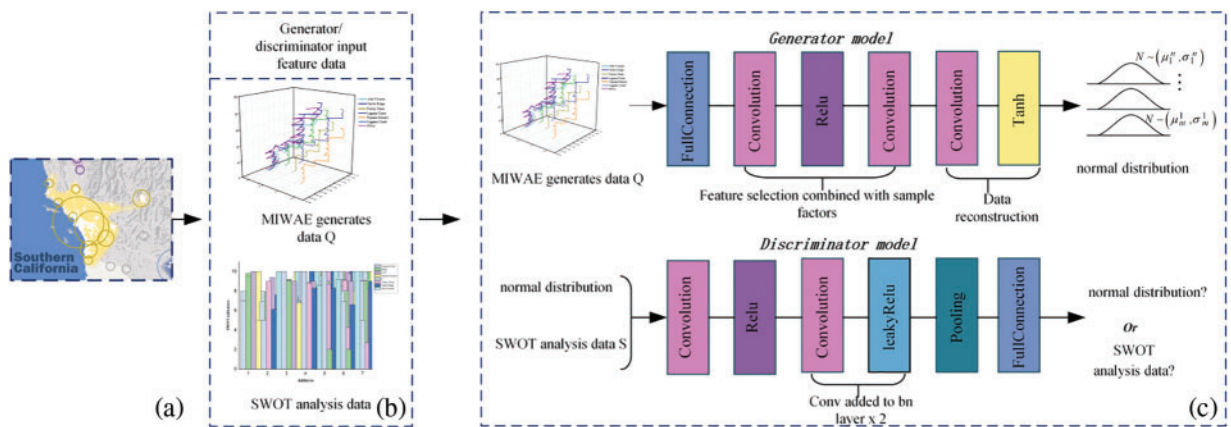


**Figure 2:** System overview of GAN networks for reconstructing environmental signals in SAE-GAN. (a) Monitoring point address location messages, i.e., data snapshots; (b) MIWAE generation data/environmental data; (c) Structure of generation model and discrimination model

In addition, we propose to incorporate an analytical model, TOPSIS, to further validate the reconstruction data.

The main contribution of this paper is fourfold:

- We propose a joint generative model called SWOT-MIWAE-GAN for environmental data reconstruction. The model seamlessly combines two popular generative models, i.e., GAN and

MIWAE, to generate features conditional on categorical data embedding after SWOT analysis. The model is capable of generating features that are similar to the real feature distribution.

- We add sample factors to add conditions to the data generation so that the final generated data is more accurately tracked on each sample data. In addition, we employ perceptual reconstruction as a fine-grained similarity metric to better capture the details and complexity of environmental features.

- We applied our methodology to the Southern California species in the United States citing SWOT analysis data to train the model, and experimented with multiple classes of loss functions as criteria, respectively. The results show that the proposed model pioneers the expansion of environmental data and achieves significant performance improvements compared to traditional methods applied to environmental data. Not only can it work in the area of species introduction, which is the role of this paper, but it can be extended to other ecological tasks.

- Our model is further validated that its data reconstruction is equally well generalized and robust in its holistic nature by the TOPSIS expertise classification assessment commonly used in the environmental data domain.

## 2 Related Work

To analyze time-varying ecological data in a more comprehensive and multidimensional way, scientific data analysis has been extensively studied. Existing research methods are based on three main categories: 1) a solution based on environmental data fusion; 2) a solution based on SWOT combined with empowered TOPSIS; and 3) a solution based on VAE add GAN reconstructed data.

### 2.1 Data Fusion

The core idea of data fusion is usually to aid in signal reconstruction by employing other classes of data. Of these, there are broad correlations between the different categories [17–20]. Yin [21] realized the integration of multiple types of data in ecosystems and biological environments by combining water quality monitoring data and biomonitoring data through the establishment of a GIS dynamic monitoring model. Raut et al. [22] proposed a distributed decision fusion framework for the ecosystems and successfully applied the fusion model to the development of intelligent systems for sustainable planning.

However, the two major bottlenecks in data fusion in the environmental category are: 1) method designers need to know which data are highly relevant to the detection target; 2) the stringent requirements for fusion controls between diversity and correlation between different categories of environmental data limit the use of data and the construction of models. In contrast, the SAE-GAN proposed in this paper fuses different categories of data by SWOT analysis and then inputs them as a single data source, which is easier to fuse and generalize. However, there is a point to note that this paper selects SWOT analysis dataset for the sake of comprehensive indicators, however, SWOT analysis usually relies on the judgment and perception of an individual or organization, which may lead to the results of the analysis being biased towards subjective evaluation, therefore, please ensure that the SWOT data analysis is authoritative when adopting textual methods.

SWOT data preprocessing part: first of all, the collection of data through the positive and negative factor analysis, we will analyze the data collated into a matrix form and normalized to [0, 10] between the sample missing in the sample eigenvectors according to the actual development of the data considerations to take 0 or the mean value. Subsequently load and randomly disrupt the data input to the VAE-GAN model via the data loader and add random noise, if other noise parameters are

present in the data, we will add additional noise to the encoder/generator model. The overall data preprocessing process is shown in Fig. 3.

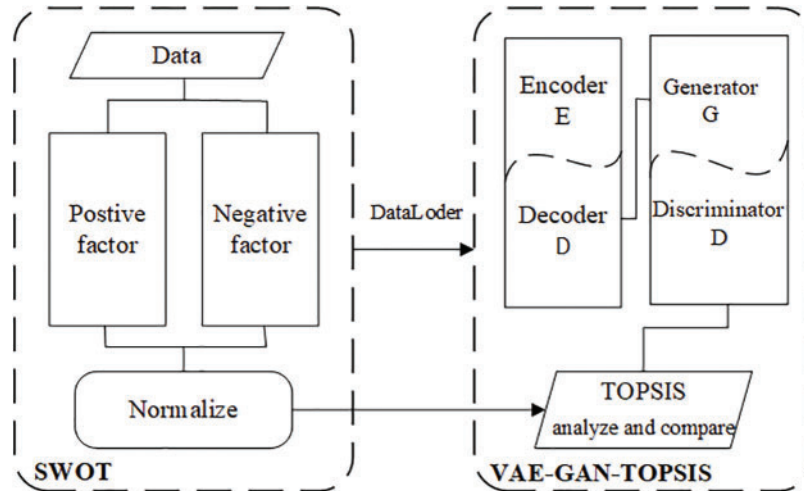


Figure 3: Overall data process

## 2.2 SWOT-TOPSIS

SWOT analysis is a good model for data analysis when collecting and analyzing multiple categories of ecological data while integrating different categories of data in a holistic manner [23–25]. In this case, SWOT is combined with TOPSIS in terms of positive and negative vectors to better capture the characteristics and patterns of the data through similarity ranking decisions [23–25]. TOPSIS is the conversion of internal and external factors in SWOT into numerical indicators. It should be incorporated into TOPSIS evaluation system to effectively achieve strategic objectives [26]. It is also widely used in the field of environment [27] and species domains [23].

As can be seen, TOPSIS was able to further optimize the SWOT data and rank the results for vectorial analysis. Based on this, the SAE-GAN proposed in this paper, as a data vector-driven model based on modeling reconstruction, is introduced into TOPSIS for further examination, to determine the accuracy of their reconstructed data for better generalization to other environmental domains.

## 2.3 VAE-GAN

In recent years, advances in deep learning techniques have demonstrated the great potential of CNN networks in extracting data features [28]. Meanwhile, data generation models based on Convolutional Neural Network (CNN), to show strong advantages and are used in a wide range of application areas such as diverse sample generation [29], generating realistic samples [30], learning data distributions [31], and unsupervised feature learning [32]. Among them, VAE accurately generates samples by mapping the original data space through the encoded latent space [33], and GAN improve its performance through mutual adversarial training between the generators and the discriminators [34], each of which has its own advantages and both of which have been widely used.

The combination of the two architectures generates samples that are even more diverse and controlled [12], but complex architectures have some drawbacks. 1) Overfitting and limited scalability for missing data or insufficient datasets. 2) Difficult to generate data based on a particular sample.

SAE-GAN uses an improved encoder MIWAE to introduce a hybrid loss function with multiple interpolations to improve the processing data capability. At the same time, the GAN network training process introduces the sample factor to make its generated sample data closer to specified sample characteristics, to improve the precision of data generation and accuracy of analysis.

### 3 Basic Definitions

In general, the ecological environment development data consists of different categories, in which the positive factors (air, soil, habitat quality; ecological region protection area and status), negative factors (extreme weather and vegetation succession, etc.; land competition and human damage) are difficult to analyze correspondingly, so the ecological environment data after SWOT analysis is more convenient to analyze the sampling and data integration. For ease of presentation, we represent the SWOT analyzed data as two-dimensional analyzed data, divided into matrices, which are defined as analyzed samples for subsequent reconstruction simulations.

**Definition 1** (Analyzed data): *The results of the SWOT analysis data  $x_i$  are represented by a matrix, which records sampling data from ecological surveys within a region.*

**Definition 2** (Generated data): *Firstly, the original environmental data is recorded as  $x_i$ , after SWOT analysis, the original data is used to generate new data  $Q$  through VAE, and finally, the two are trained against each other by GAN network to finally output the reconstructed data  $q_i$ .*

**Definition 3** (TOPSIS validation): *Defining positive and negative vectors through weights, to validate the timeliness and real-time performance of reconstructed data in practical applications.*

Our goal: Given SWOT analysis environment data  $x_i$ , generate data  $q_i$  by coding complementary in Eq. (1), two mutually generating confrontations. Our goal is to use the reconstructed corresponding sample dataset tested by TOPSIS to compensate for the current lack of data on ecosystem development, for subsequent modeling and simulation predictions.

$$\max \min \sum_{i=1}^N \log p\theta (x^{(i)}) \quad (1)$$

Therefore, we will illustrate in Section 4 that the reconstructed data approximates the original environmental data  $q_i$ , and serves as supplementary data  $x_i$  for the next data reconstruction.

## 4 Proposed Joint Model

### 4.1 Problem Setting

At present, the ecological environment data development still has the problem of difficult development and insufficient sample data, Therefore, data reconstruction is attempted for fewer datasets, and the SAE-GAN reconstruction model is established through experimental comparison.

We first use the data  $Q$  generated by VAE as the input data for generator  $G$  in the next GAN model, and generate Gaussian-like samples after generator training, meanwhile, we input the original data  $x_i$  into the discriminator  $D$ , and then the Gaussian-like samples and the original data are trained by the GAN network generative confrontation training, and the network learns the mapping relationship between the Gaussian-like samples and the original data, and ultimately generates the reconstructed data with the similar relationship to the reconstructed data, which can be used to supplement the required ecological data.

## 4.2 MIWAE-GAN Based Generative Modeling

The main innovations of the SAE-GAN reconstruction model are the introduction of sample factors  $sf$  in the VAE and the mutual adversarial learning of input data within two types of simulators ( $G, D$ ) in the GAN network. The combination of the two can generate new data that is more comprehensive and connected for practical use. We therefore further elaborate the innovation by means of a flowchart and specific explanations, as shown below.

As shown in Fig. 2, our joint generative model seamlessly couples the MIWAE and GAN. Below, we will first outline the different components of the overall generative model, includes adding sample factors. This is followed by a detailed description of the TOPSIS analysis model that further tests the accuracy of the generated data.

Overview of Joint Generation Models: Our proposed generative model has the following components: 1) encoder  $E$ , 2) decoder  $D^1$ /generator  $G^1$ , and 3) discriminator  $D$ . The encoder  $E$  captures the intrinsic structure of the  $x_i$  feature and maps the real feature into the potential space. The generator  $G$  is then reconstructed in the potential representation and decoded into the feature space. In the following, we will elaborate on the principles and loss functions between the different models.

### 4.2.1 MIWAE Model

First, MIWAE is a deep generative model based on the incorporation of a variational autoencoder (VAE) into the Mutual Information (MI) loss function Eq. (2), whose core idea is to learn effective hidden representations by maximizing the interaction information between the input variables and the hidden variables [35]. Utilizing mutual information as a learning objective helps to learn the feature representation better. Subsequent ablation experiments were able to validate our choice. the MIWAE data generation model is shown in Algorithm 1. The following is a specific explanation of the algorithm:

$$Eq(z|x) [\log p(x|z)] \quad (2)$$

MIWAE first constrain the direction of the reconstructed data generation by computing the negative log-likelihood loss between the input  $x$  and the reconstructed output  $p(x|z)$ .

Then the encoder  $E$  in MIWAE transcodes the feature information of the sample into a Gaussian-like distribution  $d_i$  and outputs the mean  $\mu_i$  and standard deviation  $\sigma_i$  as the encoded result code. Then a randomly selected value  $z_i$  from the perfect Gaussian distribution  $d_i$  constructed from the  $\mu_i$  and  $\sigma_i$  which is fed to the decoder.

Instead of outputting an implicit representation of the original data directly, the encoder outputs the mean  $\mu_i$  and standard deviation  $\sigma_i$  distilled from the original data. After that, a normal distribution with mean  $\mu_i$  and standard deviation  $\sigma_i$  is established, and the implicit  $z$  is drawn from this normal distribution, and then the implicit representation  $z$  is input to the decoder for decoding, as summarized in Algorithm 1, which summarizes the detailed training process of MIWAE.

In order to present our model more clearly, the following describes the loss function, the overall structure, and the sample factors in turn, respectively:

Loss Function: The loss function in MIWAE is shown in Eq. (3). Where Kullback-Leibler (KL) table loss dispersion is a measure of the two sets of data distribution, is the difference between the measure, when the two sets of data distribution is closer, KL dispersion will be smaller, and vice versa,

KL dispersion will be larger, writing Eq. (4).  $\phi$  is the encoder parameter and  $\theta$  is the decoder parameter.

$$L(\theta, \phi; x, z) = E_{z \sim q_\phi(x|z)} [\log p^\theta(x|z)] - D_{KL}(q_\phi(z|x) \| p(z)) \quad (3)$$

$$KL_i = -\frac{1}{2} \sum_{i=1}^N (1 + \log(\sigma_j^2) - \sigma_j^2 - \mu_j^2) \quad (4)$$

The goal of encoding is to output data that is highly similar to the original data, so the loss function of an encoder usually includes Reconstruction Loss to measure the input and output difference portion. In our experiments, in order to refine the generation criteria and test the results, the four loss functions including KL dispersion, Regression Loss (RL), Mean Squared Error (MSE), Mean Absolute Error (MAE) are chosen to work together in Eqs. (5)–(7), bringing in the loss function formula as in Eq. (8).

$$L = -E_-(x \sim D) [\log p(x)] + KL[q(z|x) \| p(z)] \quad (5)$$

$$MSE = \frac{1}{m} \sum_{i=1}^m (y_i - \hat{y}_i)^2 \quad (6)$$

$$MAE = \frac{1}{n} \sum_{i=1}^n |\hat{y}_i - y_i| \quad (7)$$

$$L(\theta, \phi) = \frac{1}{m} \sum_{i=1}^M (x_i - \hat{x}_i)^2 - \frac{1}{2m} \sum_{i=1}^M \sum_{j=1}^K (1 + \log(\sigma_j^2) - \sigma_j^2 - \mu_j^2) \quad (8)$$

Structure: The overall structure of MIWAE is shown in Table 1: Encoder  $E$  serves as the data generation model for MIWAE through a two-layer CNN for feature extraction and nonlinear mapping, respectively. Both subsequent layers use a linear layer for nonlinear transformation to better capture the higher order features of the data. After receiving the  $E$  information, the decoder  $D^1$  further amplifies the feature mapping through one linear layer, two layers of transposed convolution, and finally the sigmoid function activation function is used to restrict the output value to the  $[0, 1]$  interval.

Sample Factor: In order to make the generated data samples arbitrarily close to the environmental samples in a particular region  $x_i$ , we introduce a sampling factor  $sf_{x_i}$  for the generator model definition, as shown in Eq. (9).

The sample factor acts in the model generator to add a dimension to the generator, splicing the sample factor to the input with a dimension that is consistent with the number of input samples and features. Reconstructed data characterized by a particular sample is generated by adjusting the parameters of the sample factor in the generator by setting all parameters except the tracking sample to 1.

$$\min_{x_i} \leq sf \in x_i \leq \max_{x_i} \quad (9)$$



**Table 1:** MIWAE's structural setup

Encoder $E$		
Layers	Parameters	Output shapes
Input	/	$7 \times 16 \times 3$
conv-1 + ReLU	$I_1 = 1, O_1 = 16, K_1 = 3, S_1 = 2, P_1 = 1$	$7 \times 32 \times 7$
conv-2 + ReLU + Flatten	$I_2 = 16, O_2 = 32, K_2 = 3, S_2 = 2, P_2 = 1$	$7 \times 32 \times 7$
Linear + ReLU	$I_3 = 32 \times 13, O_3 = 256$	$7 \times 256$
Linear	$I_4 = 256, O_4 = 2 \times 49$	$7 \times 2 \times 49$
Decoder $D^1$		
Layers	Parameters	Output shapes
Input	/	/
Linear + ReLU	$I_1 = 49, O_1 = 256$	$7 \times 256$
Linear + ReLU	$I_2 = 256, O_2 = 32 * 13$	$7 \times 32 \times 13$
Unflatten	$I-BS'_3 = 2, O-BS'_3 = (32, 13)$	$7 \times (32, 13)$
Conv-Transpose + ReLU	$I_4 = 32, O_4 = 16, K_4 = 3, S'_4 = 2, P'_4 = 1$	$7 \times 16 \times 25$
Conv-Transpose	$I_5 = 16, O_5 = 1, K_5 = 3, S'_5 = 2, P'_5 = 1$	$7 \times 1 \times 49$
Sigmoid	/	Scalar

#### 4.2.2 GAN Model

We combine the VAE output data with the reconstructed data trained by the GAN network, and the reconstructed data with better accuracy will be generated through mutual adversarial learning, and the specific structure of its GAN network is shown below:

A GAN network is a network structure in which the generator  $G$  and the discriminator learn to compete with each other to generate artificial samples that are indistinguishable from real samples by learning complex distributions among the data [34]. The special cross-entropy formula for GAN in the generator-discriminator involution relation is shown in Eq. (10). Which denotes the result judged by the discriminator  $D(x_i)$  on the real data  $x_i$  in the generation which is based on the fake data generated by  $G(z_i)$ .  $D(G(z_i))$  denotes the result judged by the discriminator on the fake data  $G(z_i)$ . The adversarial training method is described in Algorithm 2.

$$V(D, G) = \frac{1}{m} \sum_{i=1}^m [\log D(x_i) + \log (1 - D(G(z_i)))] \quad (10)$$

Similarly, the next specifics are presented in terms of the loss function, and the overall structure, respectively:

Loss Function: for the discriminator  $D$  loss as in Eq. (11), we expect that the outputs  $D(x_i)$  on the true samples are all infinitely close to 1, while the outputs  $D(G(z_i))$  on the false samples are all infinitely close to 0. For the generator  $G$ , on the other hand, it cannot affect  $D(x_i)$ , only  $D(G(z_i))$ , so only the second half of the loss is relevant to the generator, and hence there is Eq. (12) for the generator.

When both are combined, the loss  $V$  is shown in Eq. (13).

$$Loss_D = \frac{1}{m} \sum_{i=1}^m [\log D(x_i) + \log(1 - D(G(z_i)))] \quad (11)$$

$$Loss_G = \frac{1}{m} \sum_{i=1}^m [\log(1 - D(G(z_i)))] \quad (12)$$

$$\min_G \max_D V(D, G) = E_{x \sim p} [\log D(x)] + E_{z \sim p_z} [\log(1 - D(G(z)))] \quad (13)$$

Structure: The specific structure of the GAN network is shown in Table 2: learning data generation using CNNs in end-to-end mapping from coarse inputs to ground truth Kang et al. obtained good practical results in environmental data generation [20]. Inspired by this, we choose three-layer CNN as the generative model in the generator to realize the mapping relationship, but before that, due to the low number of samples in the input data, we choose to first combine the input noise with other features through the FC layer to generate a more advanced feature representation.

**Table 2:** GAN's structural setup

Generative model $G$		
Layers	Parameters	Output shapes
Input	/	/
fc1	$n_{FI} = 256$	$7 \times 256 \times 1$
conv-1 + ReLU	$I_2 = 1, O_2 = 46, K_1 = 3, S_1 = 1, P_1 = 1$	$7 \times 64 \times 256$
conv-2	$I_3 = 64, O_3 = 128, K_2 = 3, S_2 = 1, P_2 = 1$	$7 \times 128 \times 256$
conv-3	$I_4 = 128, O_4 = 49, K_3 = 3, S_3 = 1, P_3 = 1$	$7 \times 49 \times 256$
tanh	$I_4 = 128, O_4 = 49$	Scalar
Discriminative model $D$		
Layers	Parameters	Output shapes
Input	/	$7 \times 49 \times 1$
conv-1 + bn + ReLU	$I_1 = 49, O_1 = 64, K_1 = 3, S_1 = 1, P_1 = 1$	$7 \times 64 \times 1$
conv-2 + bn + leakyReLU	$I_2 = 64, O_2 = 128, K_2 = 3, S_2 = 1, P_2 = 1$	$7 \times 256 \times 1$
conv-3 + bn + leakyReLU	$I_3 = 128, O_3 = 256, K_3 = 3, S_3 = 1, P_3 = 1$	$7 \times 256$
pool	$I_4 = 32, O_4 = 16, K_4 = 3, S_4 = 2, P_4 = 1$	$7 \times 256$
fc1	$n'_{FI} = 256$	7, 1

In the mapping, we approximate the corresponding environmental data  $x_i$  given  $q_i$  as input and the output class Gaussian distribution  $d_i$ , i.e.,  $x_{opt} = G(d_i)$ . As shown in Table 2, the  $G$  model consists of three convolutional layers that are connected in layers to represent different operations: 1) feature extraction and representation; 2) nonlinear mapping; and 3) reconstruction. Where the kernel size, step size, and padding of the convolutional layer are denoted by  $f_1, f_2, f_3; s_1, s_2, s_3$  and  $p_1, p_2, p_3$ , respectively. All three CNN layers are nonlinearly transformed using the ReLU activation function. The final layer of the generator model uses a Tanh activation layer to restrict the output values to between  $(-1, 1)$ .

For the discriminator model, we use a structure similar to  $G$ , with two linear layers followed by two transposed convolutional layers. All of them use ReLU activation function. Finally, the features extracted from the convolutional layers are converted into scalar values by means of a fully connected layer, which determines whether the samples are real or generated.

### 4.2.3 TOPSIS Model

The TOPSIS model of superior and inferior programs is a comprehensive evaluation method that makes full use of the information in the raw data, and its results accurately reflect the indicator gaps [25]. In this study, we constructed a TOPSIS model by combining the data generated by the generator with the  $sf_{x_i}$  with the corresponding matrix of raw environmental data ( $sf_{x_i}$  adjusted to the data of different environmental addresses in  $x_i$ ) and used the difference method  $(1 - x)$  to transform the negative indicators in the data metrics into positive indicators. The transformed data matrix is denoted, and the formula is shown in Eq. (14). Next, the raw data are normalized with the normalization formula in Eq. (15).

$$Z_{ij} = -\frac{X_{ij}}{\sqrt{\sum_{k=1}^n (X_{ik})^2}} \tag{14}$$

$$Z = \begin{pmatrix} z_{11} & z_{12} & \cdots & z_{1p} \\ z_{21} & z_{22} & \cdots & z_{2p} \\ \vdots & \vdots & \ddots & \vdots \\ z_{n1} & z_{n2} & \cdots & z_{np} \end{pmatrix} \tag{15}$$

TOPSIS calculates the distance between the evaluated and the optimal and worst values in Eqs. (18) and (19) based on the vector of optimal and worst values given in Eqs. (16) and (17), where the weights are determined using the entropy weighting method Eq. (20). The robustness and generalizability of the reconstructed data is further verified by comparing it with the original data  $x_i$  that has not been combined with the reconstructed data after evaluation by the TOPSIS model, and the overall evaluation process is shown in Fig. 4.

$$z^+ = \max_{nj} (z_1^+, z_2^+, \dots, z_p^+) \tag{16}$$

$$z^- = \min_{nj} (z_1^-, z_2^-, \dots, z_p^-) \tag{17}$$

$$D_i^+ = \sqrt{\sum_{j=1}^m (z_{ij} - Z_j^+)^2} \tag{18}$$

$$D_i^- = \sqrt{\sum_{j=1}^m (z_{ij} - Z_j^-)^2} \tag{19}$$

$$d_j = 1 - e_j \tag{20}$$

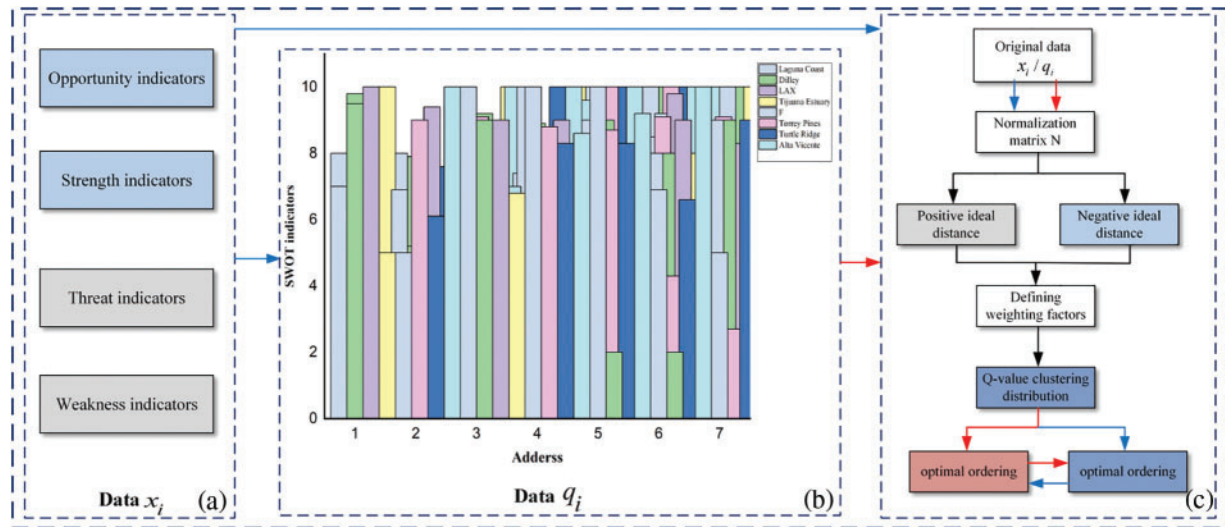


**Figure 4:** Building TOPSIS model to further validate the robustness and generalizability of reconstructed data. (a) Environmental data  $x_i$  analyzed directly; (b) Indirect analysis of data generated by MIWAE; (c) Comparison of the two ranking results

## 5 Evaluation

### 5.1 Description of the Data Set

In this paper, we analyze a sample of data using a SWOT analysis of potentially receptive sites in the field of environmental development regarding the Pacific kangaroo rat in South America [36]. The 49 categories of metrics in 7 addresses are taken for preprocessing, followed by reconstructing the data through SAE-GAN, and finally, the original data samples combined with the corresponding generated reconstructed data samples are validated through TOPSIS.

### 5.2 Experimental Setup

For the environmental sample data, we encode the environmental sample data matrix  $x_i = mn$  ( $m = 7, n = 47$ ) to generate the reconstructed data  $d_i = m, n_i$  ( $i \in 1 \sim 7$ ). Next, it will be fed to the generator and discriminator, respectively, and the performance of the signal reconstruction will be evaluated by measuring the loss values of the reconstructed signal with respect to the original signal and TOPSIS analysis.

The proposed implementation of SAE-GAN is based on CNN, TensorFlow [37], and TensorLayer [38]. All networks were trained on Google Colab v100 GPUs. The structural settings of MIWAE and GAN in SAE-GAN are shown in Tables 1 and 2, where “Conv” denotes the convolutional layer, “FC” denotes the fully connected layer, and “bn” denotes batch normalization. For network optimization, we use the Adam optimizer.

### 5.3 Performance Assessment

For SAE-GAN, as described in Section 4.1. Ecosystem development data has the problem of fewer samples, to prevent training overfitting due to the number of samples, so we use a variety of loss functions to work together to train the best reconstruction indicator data.

Based on the data  $q_i$  generated by MIWAE as mentioned in Section 4.2, the data reconstruction performance of MIWAE on the baseline method and the optimal number of iterations are tested by means of MAE, Iteration loss, RL, MI and KL evaluation metrics test model. These metrics are important tools for evaluating and optimizing the performance of data reconstruction, they help us to understand the effectiveness of the model in dealing with missing data and reconstructing ecological datasets, and to determine the optimal number of iterations to achieve the best performance. The overall performance of SAE-GAN reconstructed data is later compared by discriminator loss ( $d\_loss$ ), generator loss ( $g\_loss$ ), MSE and MAE in GAN network. Figs. 5 and 6 list the results of environmental data reconstruction, from which it can be seen that the two metrics get the best results at 50/100 iterations respectively, meanwhile, the SAE-GAN proposed in this paper achieves the best performance in environmental data reconstruction.

As described in Section 4.1, many environmental development difficulties make for sparse data volumes and small sample sizes. To prevent training overfitting, we chose multiple classes of loss functions to work together, and Figs. 5 and 6 show that the best iterations occur 50/100 times. 1) The results of Fig. 5 for RL loss, overall loss, Avg. MAE, KL scatter, and MI loss are  $13.626 \times 10^3$ ,  $15.61 \times 10^3$ , 1.96, 14.76, 0.35, the proposed MIWAE method is seen to outperform the baseline in terms of KL scatter. 2) The results of  $d\_loss$ ,  $g\_loss$ , MSE, and MAE loss in Fig. 6 are 0.0183, 0.1027,  $2 \times 10^3$ ,  $2.3 \times 10^3$ , where MSE and MAE losses were similarly better than baseline. We observe that the MSE drops off a cliff as the number of iterations increases, and we believe that multiple iterations cause training overfitting.

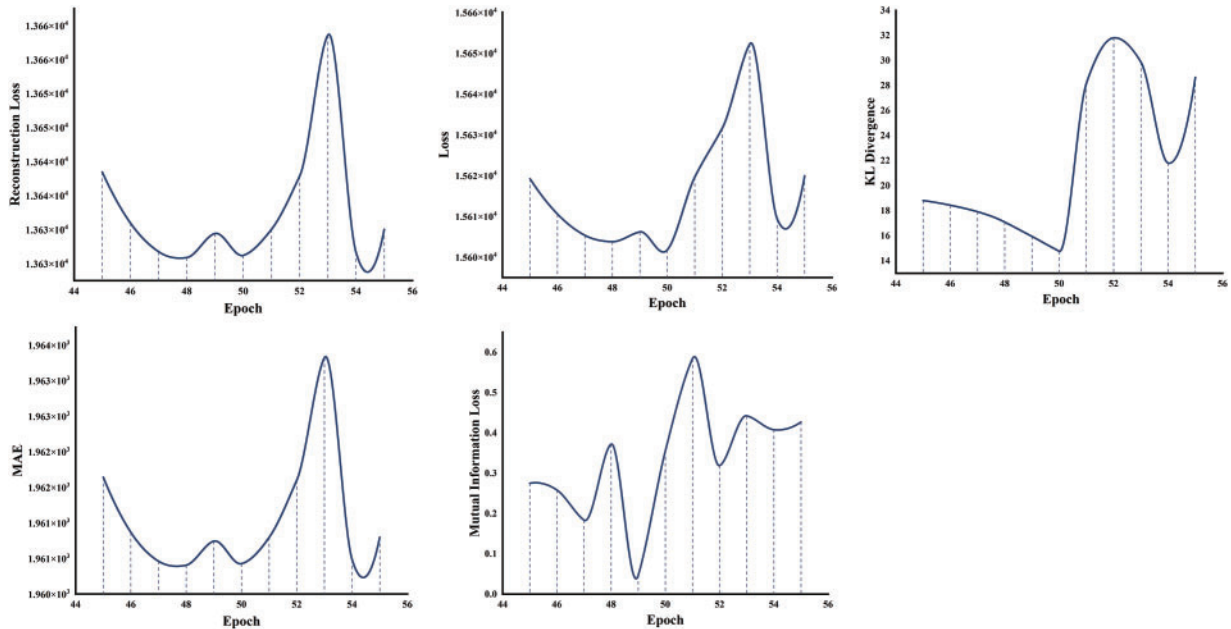


**Figure 5:** RL loss; overall loss; Avg. MAE; KL scatter; MI loss for MIWAE in SAE-GAN

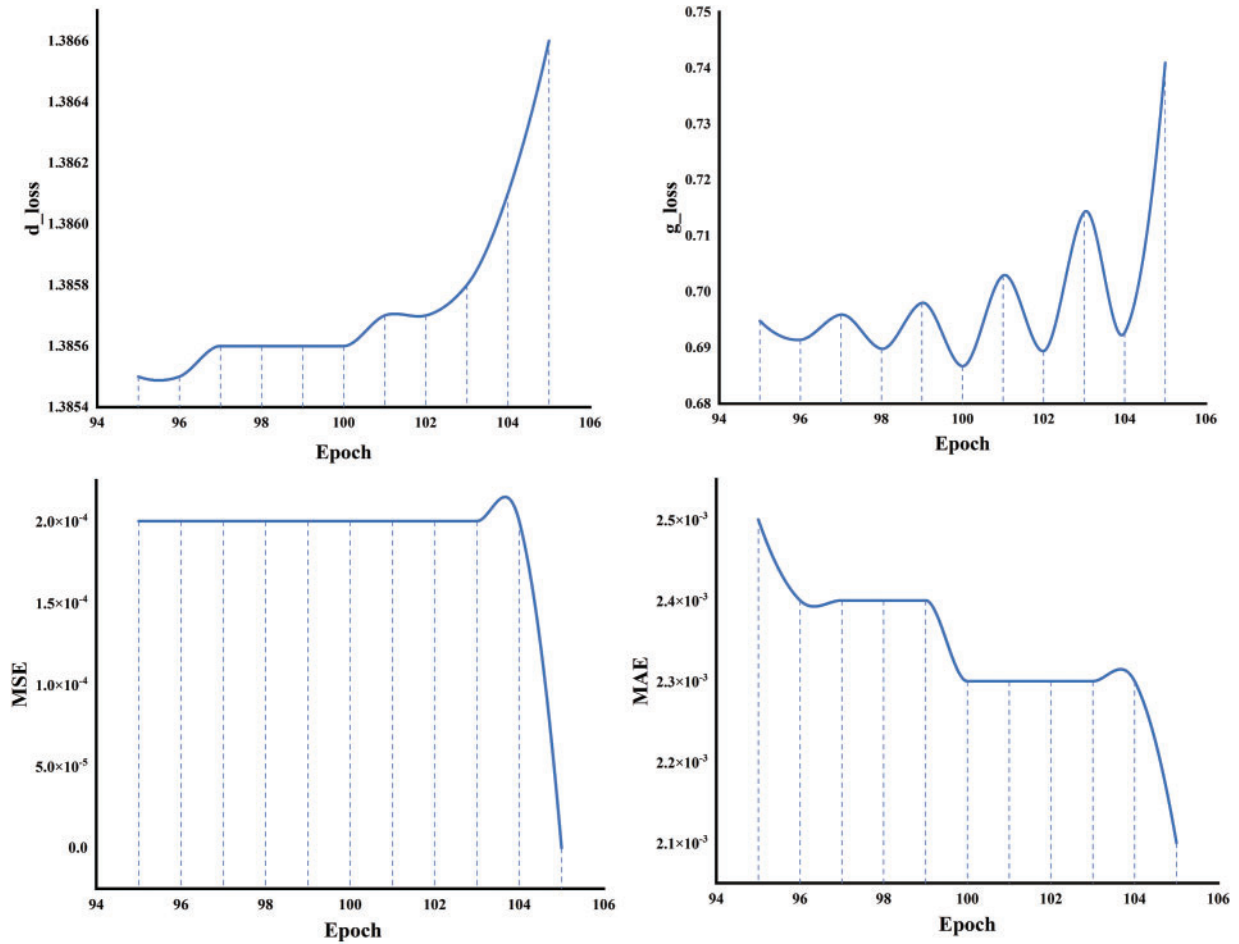


**Figure 6:** d\_loss, g\_loss; MSE; MAE loss of GAN network in SAE-GAN

---

**Algorithm 1:** MIWAE data generation methodology

---

**Input:** SWOT analysis sample  $x_i$ , feature tensor,  
maximum iterative number  $maxIter$ , weight factor,  
learning rate  $\eta$ , optimizer Adam;

**Output:** Generate data Q, The value of the KL Divergence,  
and MAE as well as Mi interaction loss values;

Mi  $\leftarrow$  Mutual Information;

Loss  $\leftarrow$  Impose a penalty term on the encoder;

Variable  $t \leftarrow 0$ ;

**while**  $t < maxIter$  **do**

    each  $x_i$  in encoder do, output Gaussian distribution  $d_i$

    add Loss  $L(\theta, \phi; x, z) = E_{z \sim q_\phi(x|z)} [\log p_\theta(x|z)] - D_{KL}(q_\phi(z|x) \parallel p(z))$

        // Impose a penalty term on the encoder and Mi Loss;

    //  $\theta, \phi$  Auto-encoder parameters;

---

(Continued)

**Algorithm 1 (continued)**


---

```

    output  $\mu_1 \cdots \mu_m \leftarrow$  average values,  $\sigma_1 \cdots \sigma_m \leftarrow$  standard deviation;
  for  $d_i \rightarrow D_i$  do
     $\begin{bmatrix} \mu_1 \\ \vdots \\ \mu_m \end{bmatrix} + \begin{bmatrix} \sigma_1 \\ \vdots \\ \sigma_m \end{bmatrix} \rightarrow \begin{bmatrix} z_1 \\ \vdots \\ z_m \end{bmatrix} \rightarrow$  perfect Normal distribution  $D_i$ ;
    // Drawing  $Z_i$  from a normal distribution.
  for  $Z_i$  in Decoder do
    Output data  $q$  and calculate MAE and Mi loss;
    // Update parameters of  $z$  with
  decoder:  $t \leftarrow t + 1$ ;
return Generate data Q, KL Loss, Mi, MAE;
```

---

**Algorithm 2: Adversarial training methods for GAN**


---

```

Input: Generate data Q, Batch size m, collection of low-/high-quality
    sensing signal pairs P, collection of impact map I, maximum iterative number maxIter,
    generator and discriminator subepochs  $G$  and  $D$ , weight factor  $\lambda$ , learning rate  $\eta$ ;
Output: Optimized parameters of generative network
     $\phi_G$ , and optimized parameters of discriminative network  $\phi_D$ , Loss.
 $\phi_G, \phi_D \leftarrow$  Small random values;
Loss  $\leftarrow$  g_loss, d_loss, MSE, MAE;
for number of training iterations do
  for  $k$  steps do
    Sample minibatch of  $m$  noise samples  $\{z^{(1)}, \dots, z^{(m)}\}$  from noise prior  $p_g(z)$ .
    Sample minibatch of  $m$  examples  $\{x^{(1)}, \dots, x^{(m)}\}$  from data generating distribution  $p_{data}(x)$ .
    Update the discriminator by ascending its stochastic gradient:
      
$$\nabla_{\theta_d} \frac{1}{m} \sum_{i=1}^m [\log \phi_D(x^{(i)}) + \log(1 - \phi_D(\phi_G(z^{(i)})))]$$

  end for
    Sample minibatch of  $m$  noise samples  $\{z^{(1)}, \dots, z^{(m)}\}$  from noise prior  $p_g(z)$ .
    Update the generator by ascending its stochastic gradient (improved objective):
      
$$\nabla_{\theta_g} \frac{1}{m} \sum_{i=1}^m \log(\phi_D(\phi_G(z^{(i)})))$$

return  $\phi_G, \phi_D$ ;
```

---

**5.4 TOPSIS Test Analysis**

As mentioned in [Section 4.2](#), in order to further test whether the reconstructed data in its entirety can be used for subsequent modeling simulation predictions, we analyze the results of each sample in the original environmental data  $x_i$  individually by TOPSIS and then compare them with the data generated by SAE-GAN after combining them by TOPSIS analysis. Its analysis results are shown in [Table 3](#), and the TOPSIS analysis results after adding the reconstructed data are consistent with the original results, which verifies the reconstruction accuracy.

**Table 3:** TOPSIS analysis comparison

Norm	Positive ideal solution distance	Negative ideal solution distance	Composite score index	Combining reconstructed data (D+)	Combining reconstructed data (D-)	Reconstructed data (score index)	Arrange in order
LAX	0.57582076	0.73849507	0.56188555	0.55854247	0.68660689	0.55142532	1
Tijuana estuary	0.60833461	0.70017705	0.53509424	0.65527205	0.58559769	0.47192519	2
Alta vicente	0.6005932	0.68927405	0.53437596	0.69990852	0.55755838	0.44339806	3
Torrey pines	0.66530357	0.63915284	0.48997639	0.72534289	0.52228092	0.41862052	4
Dilley	0.72825653	0.53136242	0.42184378	0.69702325	0.48932224	0.41246184	5
Laguna coast	0.77935812	0.5346117	0.40686756	0.73706779	0.51322836	0.41048543	6
Turtle ridge	0.77491456	0.48886518	0.38682783	0.78118011	0.42123606	0.35032468	7

### 5.5 Ablation Study of ESR-GAN

Here we conduct an extensive ablation study to evaluate how the SAE-GAN framework affects the reconstruction results of environmental data. The experiments are conducted in terms of uniformity and diversity, respectively.

Uniformity test: As mentioned above, the solution pipeline of SAE-GAN consists of three main parts: 1) encoder  $E$ ; 2) decoder  $D^1$ , generator  $G$ ; 3) discriminator  $D$ , while we combine multiple classes of loss functions to jointly verify the reconstruction accuracy. Therefore, we perform ablation in two ways: 1) the encoder removes the MI loss and 2) the end-to-end output using either the encoder-decoder or generator-discriminator network alone, i.e., removing a portion of the overall frame condition. From [Table 4](#), we observe that each ablation of SAE-GAN leads to worse signal reconstruction performance. These results show that the SAE-GAN framework can effectively improve the quality of reconstructed data.

**Table 4:** Ablation study

Experimental methods	Loss	Reconstruction loss	KL divergence	Mutual information loss	d_loss	g_loss	MSE	MAE
SAE-GAN	15,601.7471	13,626.2051	14.7594	0.3558	1.3834	0.7048	0.1034	0.2427
VAE LOSS	15,628.2773	15,628.2773	18.1834	18.1834	/	/	/	/
Encoder-Decoder only	15,601.7471	13,626.2051	14.7594	0.3558	/	/	/	/
Generator-discriminator only	/	/	/	/	1.3856	0.6867	0.0002	0.0023

Diversity of Test Cases: As stated in the introduction above, in order to understand the advantages of SAE-GAN over other common generative adversarial networks in terms of diversity of test cases, AE, GAN, WGAN, and DCGAN were chosen as comparison models for the experiment. In some tests, DCGAN, WGAN usually do not directly calculate the reconstruction loss, KL scatter and MI loss, so we uniformly adopt MSE, MAE as the evaluation index of this ablation experiment. From [Table 5](#), it can be seen that our constructed model possesses better prediction accuracy and indexes compared with other models.



**Table 5:** Diversity experiments

Evaluation indicators	MSE	MAE
<b>Other works</b>		
AE	0.1494	0.2517
GAN	44.2968	6.1034
DCGAN	40.3362	5.7864
AE-GAN	0.0437	0.1664
VAE-WGAN	6.6972	52.2040
<b>Our's</b>		
SAE-GAN	<b>0.0183</b>	<b>0.1027</b>

### 5.6 SAE-GAN Extension Study

A practical framework for environmental data reconstruction should have the ability to generalize to handle multiple types of data and adapt to various states of reality such as integrated assessment. In this paper, the sampling state refers primarily to the number of monitoring sites and their corresponding spatial layout. We analyzed the data through SWOT and input environmental data reconstruction. The data is generated by two overlays and a lot of experiments are conducted, the final result verifies that SAE-GAN has better training accuracy and generalization compared to other data reconstruction models.

However, the SAE-GAN model established in this paper also possesses certain limitations, as mentioned in [Section 2.1](#), SWOT analysis is highly subjective and may bias the analysis results. Meanwhile, although SAE-GAN can follow up the real-time change data of the ecological environment by adjusting the SWOT parameters, SWOT belongs to the comprehensive integration analysis, and the real-time change parameters of a certain point may have an impact on the overall analysis results. For the above problems, we consider incorporating certain noise (influence parameters) and acting on larger datasets in future research, as well as incorporating other features of generative adversarial networks, such as domain transformation and conditional generation, which can also be introduced into the model.

Adaptation of SAE-GAN models to other environmental challenges can be continuously explored in future research by optimizing the algorithm and loss function to will improve the stability of training and generation quality. In addition, investigating new network structures and techniques may reduce training time and computational resource requirements. Future research will also need to consider data privacy and ethical issues to ensure that the application of the model does not violate individual privacy or cause adverse social impacts and, at the same time, ensure that the data generated respect the principles of ecological diversity and sustainability.

## 6 Conclusion

In this paper, we propose a new generative model-based framework, SAE-GAN, for reconstructing environmental signals by sparse and homogeneously distributed sampling. By combining two popular generative models and expanding the loss function action rate, the model can synthesize high-quality features with elemental similarity and overall similarity to real features. Based on the problem of

differences in sampled data categories, the proposed SAE-GAN model incorporates sample factors to provide complementary conditions for generating data and obtains better performance than the environmental data techniques commonly acted upon. Multi-class loss function detection and TOPSIS model analysis ranking as well as ablation experiments demonstrated that our model can generate data features similar to the original data for use in problems that cannot be further analyzed for prediction due to lack of sufficient environmental data. Future research will act on larger datasets combined with more advanced generative modeling architectures to accommodate richer and more complex ecological data by facilitating model generation. This includes models capable of handling both temporal and spatial data, which are critical for capturing the dynamics of biological patterns and environmental change.

**Acknowledgement:** The editors and anonymous referees whose comments and recommendations have helped to improve this work are greatly appreciated by the authors. The authors would like to express their gratitude for the guidance and support provided by the research group.

**Funding Statement:** This work was supported by the Fundamental Research Funds for the Liaoning Universities (LJ212410146025).

**Author Contributions:** Shuqiao Liu: Methodology, Data Curation, Writing—Original Draft. Zhao Zhang: Conceptualization, Supervision, Reviewing and Editing. Hongyan Zhou: Reviewing and Editing. Xuebo Chen: Reviewing. All authors reviewed the results and approved the final version of the manuscript.

**Availability of Data and Materials:** Data and materials are available upon request.

**Ethics Approval:** Not applicable.

**Conflicts of Interest:** The authors declare no conflicts of interest to report regarding the present study.

## References

- [1] X. Jin, Y. Li, J. Wan, X. Lyu, P. Ren and J. Shang, “MODIS green-tide detection with a squeeze and excitation oriented generative adversarial network,” *IEEE Access*, vol. 10, no. 6, pp. 60294–60305, 2022. doi: [10.1109/ACCESS.2022.3180331](https://doi.org/10.1109/ACCESS.2022.3180331).
- [2] T. Li, L. Kong, X. Yang, B. Wang, and J. Xu, “Bridging modalities: A survey of cross-modal image-text retrieval,” *Chin J. Inf. Fusion*, vol. 1, no. 1, pp. 79–92, 2024. doi: [10.62762/CJIF.2024.361895](https://doi.org/10.62762/CJIF.2024.361895).
- [3] S. H. Ali, I. Ullah, S. A. Ali, M. I. UL Haq, and N. Ullah, “A cyber-physical system based on On-Board Diagnosis (OBD-II) for smart city,” *IECE Trans. Intell. Syst.*, vol. 1, no. 2, pp. 49–57, 2024. doi: [10.62762/TIS](https://doi.org/10.62762/TIS).
- [4] S. Sun, L. Mu, R. Feng, L. Wang, and J. He, “GAN-based LUCC prediction via the combination of prior city planning information and land-use probability,” *IEEE J-STARS*, vol. 14, pp. 10189–10198, 2021. doi: [10.1109/jstars.2021.3106481](https://doi.org/10.1109/jstars.2021.3106481).
- [5] A. Varghese, M. Jawahar, and A. A. Prince, “Transfer learning-based rich feature analysis on leather images for species prediction,” in *2023 10th Int. Conf. Signal Proces Integrat Networks (SPIN)*, Noida, India, 2023, pp. 301–305. doi: [10.1109/SPIN57001.2023.10117459](https://doi.org/10.1109/SPIN57001.2023.10117459).
- [6] X. Zhao, R. Liu, and Y. Ma, “Hyperspectral remote sensing reflectance data augmentation method for red tide dominant species based on condition generative adversarial net,” in *2023 IEEE India Geosci. Remote Sens. Symp. (InGARSS)*, Beijing, China, May 7–10, 2023, pp. 1–4.

- [7] A. Ferchichi, A. B. Abbes, V. Barra, and M. Rhif, "Multi-attention Generative Adversarial Network for multi-step vegetation indices forecasting using multivariate time series," *Eng. Appl. Artif. Intell.*, vol. 128, 2024. doi: [10.1016/j.engappai.2023.107563](https://doi.org/10.1016/j.engappai.2023.107563).
- [8] W. Li, T. Zheng, Z. Yang, M. Li, C. Sun and X. Yang, "Classification and detection of insects from field images using deep learning for smart pest management: A systematic review," *Ecol. Inform.*, vol. 66, no. 7, 2021, Art. no. 101460. doi: [10.1016/j.ecoinf.2021.101460](https://doi.org/10.1016/j.ecoinf.2021.101460).
- [9] Y. Cai, L. Chen, X. Zhuang, and B. Zhang, "Automated marine oil spill detection algorithm based on single-image generative adversarial network and YOLO-v8 under small samples," *Mar. Pollut. Bull.*, vol. 203, no. 19, Jun. 2024, Art. no. 116475. doi: [10.1016/j.marpolbul.2024.116475](https://doi.org/10.1016/j.marpolbul.2024.116475).
- [10] M. Akbari and J. Liang, "Semi-recurrent CNN-based VAE-GAN for sequential data generation," in *2018 IEEE Int. Conf. Acoust., Speech Signal Process. (ICASSP)*, Calgary, AL, Canada, Apr. 15–20, 2018.
- [11] A. A. Aperocho, S. R. Chan, J. M. Mangali, R. J. M. Orpeza, and M. A. Purio, "Spatiotemporal pattern of mangrove forests in bulacan using satellite data fusion method and machine learning," in *IGARSS 2023—2023 IEEE Int. Geosci. Remote Sens. Symp.*, Bulacan, Philippines, 2023, pp. 6732–6735.
- [12] J. Kos, I. Fischer, and D. Song, "Adversarial examples for generative models," in *2018 IEEE Secur. Priv. Workshops (SPW)*, Toulon, France, Apr. 24–26, 2018, pp. 36–42.
- [13] L. E. Kruse, S. Kühn, A. Dochhan, and S. Pachnicke, "Monitoring data augmentation of spectral information using VAE and GAN for soft-failure identification," *J. Lightwave Technol.*, vol. 36, 2024. doi: [10.1364/OFC.2024.M31.4](https://doi.org/10.1364/OFC.2024.M31.4).
- [14] Y. Akkem, S. K. Biswas, and A. Varanasi, "A comprehensive review of synthetic data generation in smart farming by using variational autoencoder and generative adversarial network," *Eng. Appl. Artif. Intell.*, vol. 131, 2024. doi: [10.1016/j.engappai.2024.107881](https://doi.org/10.1016/j.engappai.2024.107881).
- [15] M. Arjovsky, S. Chintala, and L. Bottou, "Wasserstein GAN," 2017, *arXiv:1701.07875v3*.
- [16] A. Radford, L. Metz, and S. Chintala, "Unsupervised representation learning with deep convolutional generative adversarial networks," in *4th Int. Conf. Learn. Represent., ICLR 2016*, San Juan, Puerto Rico, May 2–4, 2016, pp. 2365–2370.
- [17] S. Vardoulakis, B. E. A. Fisher, K. Pericleous, and N. Gonzalez-Flesca, "Modelling air quality in street canyons: A review," *Atmos. Environ.*, vol. 37, no. 2, pp. 155–182, 2003. doi: [10.1016/S1352-2310\(02\)00857-9](https://doi.org/10.1016/S1352-2310(02)00857-9).
- [18] G. Lei, A. Li, J. Tan, J. Bian, and W. Zhao, "Ecosystem mapping in mountainous areas by fusing multi-source data and the related knowledge," in *IGARSS 2016—2016 IEEE Int. Geosci. Remote Sens. Symp.*, 2016. doi: [10.1109/IGARSS.2016.7729342](https://doi.org/10.1109/IGARSS.2016.7729342).
- [19] C. Trahms, Y. Wölker, P. V. K. Handmann, M. Visbeck, and M. Renz, "Data fusion for connectivity analysis between ocean regions," in *e-Science*, Salt Lake City, UT, USA, Oct. 11–14, 2022, pp. 326–335.
- [20] X. Kang, L. Liu, and H. Ma, "ESR-GAN: Environmental signal reconstruction learning with generative adversarial network," *IEEE Internet Things*, vol. 8, no. 1, pp. 636–646, 2021. doi: [10.1109/JIOT.2020.3018621](https://doi.org/10.1109/JIOT.2020.3018621).
- [21] C. Yin, "Design of dynamic monitoring system of lake ecosystem based on geographical information system," *Sustainability*, vol. 14, pp. 564–570, 2022. doi: [10.1109/icaml60083.2023.00110](https://doi.org/10.1109/icaml60083.2023.00110).
- [22] A. Raut, D. Kumar, V. K. Chaurasiya, and M. Kumar, "Distributed decision fusion for large scale IoT-ecosystem," in *2022 IEEE 15th Int. Symp. Embed. Multicore/MCSoc*, Allahabad, India, 2022, pp. 112–119.
- [23] S. M. Hosseini, M. M. Paydar, and C. Triki, "Implementing sustainable ecotourism in Lafour region, Iran: Applying a clustering method based on SWOT analysis," *J. Clean. Prod.*, vol. 329, no. 4, Dec. 2021. doi: [10.1016/j.jclepro.2021.129716](https://doi.org/10.1016/j.jclepro.2021.129716).
- [24] S. Opricovic and G. -H. Tzeng, "Compromise solution by MCDM methods: A comparative analysis of VIKOR and TOPSIS," *Eur. J. Oper. Res.*, vol. 156, no. 2, pp. 445–455, Jul. 2004. doi: [10.1016/S0377-2217\(03\)00020-1](https://doi.org/10.1016/S0377-2217(03)00020-1).
- [25] H. -S. Shih, H. -J. Shyr, and E. S. Lee, "An extension of TOPSIS for group decision making," *Math. Comput. Model.*, vol. 45, no. 7–8, pp. 801–813, Mar. 2007. doi: [10.1016/j.mcm.2006.03.023](https://doi.org/10.1016/j.mcm.2006.03.023).

- [26] W. Ning, Y. Hu, S. Feng, M. Cao, and J. Luo, "Ecological risk assessment and transmission of soil heavy metals in pastoral areas of the Tibetan plateau based on network environment analysis," *Sci. Total Environ.*, vol. 905, no. 2, 2023, Art. no. 167197. doi: [10.1016/j.scitotenv.2023.167197](https://doi.org/10.1016/j.scitotenv.2023.167197).
- [27] X. He, "Analysis of the ecological tourism development model based on SWOT," in *2014 IEEE Workshop Adv. Res. Technol. Ind. Appl. (WARTIA)*, Sep. 29–30, 2014, pp. 672–674.
- [28] J. Long, E. Shelhamer, and T. Darrell, "Fully convolutional networks for semantic segmentation," *IEEE Trans. Pattern Anal. Mach. Intell.*, vol. 39, no. 4, pp. 640–651, Apr. 2017. doi: [10.1109/TPAMI.2016.2572683](https://doi.org/10.1109/TPAMI.2016.2572683).
- [29] T. Xu *et al.*, "AttnGAN: Fine-grained text to image generation with attentional generative adversarial networks," 2017, *arXiv:1711.10485v1*.
- [30] N. Ruiz *et al.*, "DreamBooth: Fine tuning text-to-image diffusion models for subject-driven generation," 2023, *arXiv:2208.12242v2*.
- [31] M. Mirza and S. Osindero, "Conditional generative adversarial nets," in *3rd Int. Conf. Learn. Represent., ICLR 2015*, San Diego, CA, USA, May 7–9, 2015, pp. 1–7.
- [32] R. Gao *et al.*, "Zero-VAE-GAN: Generating unseen features for generalized and transductive zero-shot learning," *IEEE Trans. Image Process.*, Jan. 13, 2020. doi: [10.1109/TIP.2020.2964429](https://doi.org/10.1109/TIP.2020.2964429).
- [33] D. P. Kingma and M. Welling, "Auto-encoding variational bayes," 2013, *arXiv:1312.6114v3*.
- [34] I. J. Goodfellow *et al.*, "Generative adversarial nets," in *28th Annu. Conf. Neural Inform. Process. Syst.*, Montreal, QC, Canada, Dec. 8–13, 2014.
- [35] P. A. Mattei and J. Frellsen, "MIWAE: Deep generative modelling and imputation of incomplete data sets," in *Proc. 36th Int. Conf. Mach. Learn.*, Long Beach, CA, USA, Jun. 9–15, 2019, pp. 4413–4423.
- [36] R. Y. Chock *et al.*, "Quantitative SWOT analysis: A structured and collaborative approach to reintroduction site selection for the endangered Pacific pocket mouse," *J. Nat. Conserv.*, vol. 70, pp. 6–15, Dec. 2022. doi: [10.1016/j.jnc.2022.126268](https://doi.org/10.1016/j.jnc.2022.126268).
- [37] M. Abadi *et al.*, "TensorFlow: Large-scale machine learning on heterogeneous distributed systems," 2016, *arXiv:1603.04467v2*.
- [38] H. Dong *et al.*, "TensorLayer: A versatile library for efficient deep learning development," in *MM '17: Proc. 25th ACM Int. Conf. Multimedia*, Mountain View, CA, USA, Oct. 23–27, 2017, pp. 1201–1204.